MIMO Precoding in 802.16e WiMAX

Qinghua Li, Xintian Eddie Lin, and Jianzhong (Charlie) Zhang

Abstract: **Multiple-input multiple-output (MIMO) transmit precoding/beamforming can significantly improve system spectral efficiency. However, several obstacles prevent precoding from wide deployment in early wireless networks: The significant feedback overhead, performance degradation due to feedback delay, and the large storage requirement at the mobile devices. In this paper, we propose a precoding method that addresses these issues. In this approach, only 3 or 6 bits feedback is needed to select a precoding matrix from a codebook. There are fifteen codebooks, each corresponding to a unique combination of antenna configuration (up to 4 antennas) and codebook size. Small codebooks are prestored and large codebooks are efficiently computed from the prestored codebook, modified Hochwald method and Householder reflection. Finally, the feedback delay is compensated by channel prediction. The scheme is validated by simulations and we have observed significant gains comparing to space-time coding and antenna selection. This solution was adopted as a part of the IEEE 802.16e specification in 2005.**

Index Terms: **Feedback, multiple-input multiple-output (MIMO), orthogonal frequency division multiplexing (OFDM), precoding, transmit beamforming, vector quantization.**

I. INTRODUCTION

IEEE 802.16e [1] is a member of the family of WiMAX standards, and it is the first mobile standard that combines orthogonal frequency division multiple access (OFDMA) and multiple-input multiple-output antenna system (MIMO). Mobility support differentiates 802.16e from its predecessor 802.16d [2], which is designed for fixed wireless channels. MIMO techniques in 802.16e are categorized into open-loop and closed-loop. Space-time block code (STBC) is an open-loop diversity-only technique that requires no channel state information (CSI) at the transmitter. On the other hand, closed-loop techniques can obtain both diversity and beamforming gains at low speeds by exploiting CSI at the transmitter. Various closed-loop techniques such as antenna grouping, antennas selection, and MIMO precoding scheme are proposed and adopted by the 802.16e task group.

There are two ways of obtaining CSI for the closed-loop techniques: feedback or direct estimation via channel reciprocity. In both frequency division duplex (FDD) and time division duplex (TDD), strict channel reciprocity is difficult to maintain. While the invalidity is obvious for an FDD system, a TDD system without transmit and receive chain calibrations also fails to achieve channel reciprocity. It is due to the fact that the transmit and receive RF chains are parts of the effective downlink/uplink channels, and the chain responses with active components (PAs and LNAs) are not reciprocal. On the other hand, the CSI feedback is more challenging in 802.16e than in 802.16d because of the mobility issues such as efficiency, complexity and delay. First, the feedback overhead is not significant for fixed wireless channels, but can be prohibitive in mobility systems due to the need of frequent update. An efficient feedback scheme is essential. Secondly, 802.16e Subscriber Station (SS) supports a great variety of feedback types because it moves across cells with different antenna configurations. For example, when an SS with three receive antennas connects to a base station (BS) with three transmit antennas, the SS sends back precoding matrixes of sizes 3×1, 3×2, and 3×3 for the beamforming of 1, 2, and 3 data streams respectively according to the channel conditions. When handed over to another BS with four transmit antennas, the SS is required to feed back precoding matrixes of sizes 4×1, 4×2, and 4×3. Thirdly, the feedback delay is two frames with each frame duration of 5 ms. Even pedestrian channels can vary significantly after 10 ms, and the CSI feedback may become outdated.

It is well known that in the capacity-achieving SVD beamforming [3], only the right unitary matrix of the channel decomposition is needed at the transmitter. Various schemes [4]–[16] quantize the unitary beamforming matrix and the analysis on the quantization loss is recently reported in [16]–[18]. The quantization codebooks can be classified into two categories: Structured and unstructured. The structured codebooks [4], [5], [9]–[16] parameteriz the codewords with a few matrix operations (e.g., multiplication, Givens rotation, etc.), and thus its storage complexity is low. In contrast, the unstructured [6]–[8] codebooks optimize each codeword over a distribution of the beamforming matrix. Common optimization metrics are chordal distance [4], [6] and mutual information [8]. Unstructured codebooks typically outperform structured ones at the cost of higher storage requirements. The scheme adopted by 802.16e is a combination of both the structured and unstructured approaches to meet the storage, multi-configuration, and multi-rate requirements. The small codebooks for multiple-input single-output (MISO) channels such as 2×1 are unstructured and stored, while large codebooks for MIMO channels such as 4×2 are structured that can be efficiently computed from the stored codebooks using Householder reflection [24]. For further storage reduction, structured codebooks is derived for MISO channel 3×1 and 4×1 with 64 codewords, which are modified from [4] by relaxing the constraint of constant entry modulus. Finally, the feedback and processing delay is mitigated with a channel prediction algorithm based on Wiener filtering.

The rest of the paper is organized as follows: The system overview of the precoding for 802.16e band adaptive modulation and coding (AMC) mode is described in Section II. The channel prediction scheme is presented in Section III. The ma-

Manuscript received December 15, 2006.

Q. Li and X. E. Lin are with Intel Corporation, Santa Clara, CA, (email: {qinghua.li, eddie.x.lin}@intel.com).

J. C. Zhang is with Samsung, Richardson, TX, (email: jzhang@sta. samsung.com).

Part of this paper was presented at the task group meetings of IEEE 802.16e and IEEE VTC-spring in 2005.

1229-2370/07/$10.00 © 2007 KICS

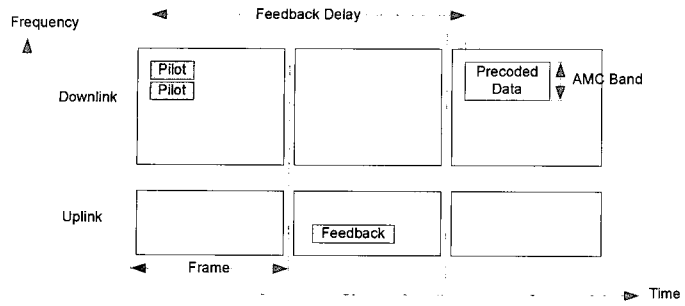

Fig. 1. Frame structure of Band AMC in FDD mode.

trix and vector codebooks are depicted in Section IV. Finally, simulation results and conclusions are presented in Sections V and VI, respectively.

II. SYSTEM OVERVIEW

The frame structure of 802.16e FDD mode is illustrated in Fig. 1. The frame is partitioned into downlink and uplink subframes. The downlink subframe consists of OFDM symbols, whose duration is 100.8 μs. The subcarrier spacing is 11.161 kHz while the number of subcarriers is scalable. The MIMO precoding is employed in Band AMC mode of OFDMA, see [19] for more details. AMC band is a resource allocation unit contiguous in frequency and time, as illustrated in the upper right corner of Fig. 1. The allocated bands are for data transmission in the downlink. The resource allocation is broadcasted one frame before the transmission frame. SS listens to the current downlink subframe header at the beginning of the frame to obtain the location of its AMC band in the next frame. One AMC band consists of 36 consecutive subcarriers, whose bandwidth is 401.796 kHz. Four training subcarriers are evenly spaced within the band. There are other training symbols, e.g., preamble and pilots in the downlink subframe.

To set up the downlink MIMO (or MISO) precoding, BS allocates a feedback channel in the uplink to an SS and requests precoding matrix feedback from the SS. The SS estimates the time varying channel matrix from the training symbols in the current and previous frames, and it feeds back the precoding matrix in the second frame. This matrix will then be used in the third frame, as shown in Fig. 1. The feedback delay is therefore 2 frames. With a frame duration of 5 ms, the feedback delay is 10 ms.

We assume a block fading model where the channel is fixed over each frame and varies across frames. The received baseband signal vector at SS is modeled as

$$\mathbf{y}(i_c,t) = \mathbf{H}(i_c,t)\underbrace{\mathbf{V}(i_c,t)\,\mathbf{s}(i_c,t)}_{\mathbf{x}(i_c,t)} + \mathbf{n}(i_c,t) \qquad (1)$$

where i_c and t are the indexes of subcarrier and frame respectively; $\mathbf{H}(i_c,t)$ is the $N_r \times N_t$ channel matrix on the i_cth subcarrier in the tth frame; $\mathbf{x}(i_c,t)$ is the $N_t \times 1$ transmitted, precoded signal vector; $\mathbf{n}(i_c,t)$ is the complex, independent and identically distributed (i.i.d.) additive white Gaussian noise (AWGN) with zero mean and variance σ^2 for each entry; $\mathbf{V}(i_c,t)$ is the $N_t \times N_s$ orthogonal precoding matrix[1]; $\mathbf{s}(i_c,t)$ is the $N_s \times 1$ signal vector whose entries are QAM symbols; N_s is the number of spatial streams. The entry of $\mathbf{H}(i_c,t)$ is i.i.d. circularly symmetric, complex Gaussian random variable with zero mean and unit variance.

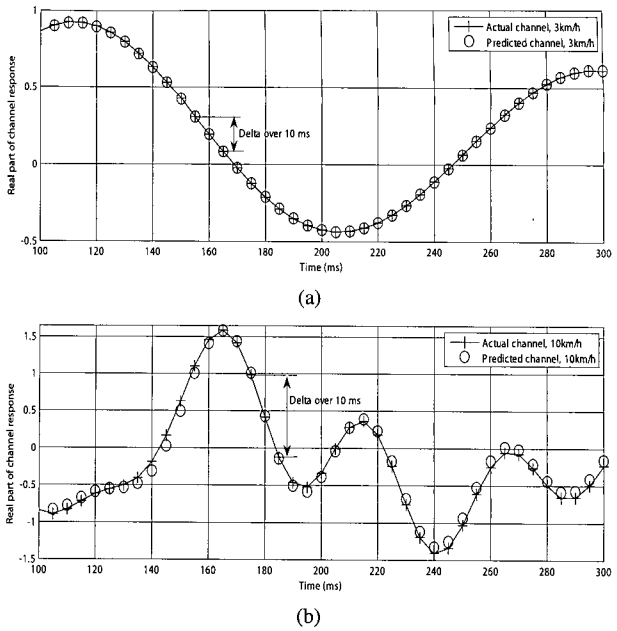

Fig. 2. Time varying fading channels and the predicted channel responses for mobile speeds: (a) 3 km/h, (b) 10 km/h.

The SS selects the precoding matrix $\mathbf{V}(i_c,t+2)$ from a codebook at frame t after observing the channels $\mathbf{H}(i_c,t)$, $\mathbf{H}(i_c,t-1),\cdots,\mathbf{H}(i_c,1)$. The index of $\mathbf{V}(i_c,t+2)$ with respect to the codebook is sent back to the BS at frame $t+1$. The BS obtains $\mathbf{V}(i_c,t+2)$ from the same codebook using the fed back index and conducts precoding, $\mathbf{V}(i_c,t+2)\,\mathbf{s}(i_c,t+2)$, at frame $t+2$. Note that there are differences between $\mathbf{H}(i_c,t)$ and $\mathbf{H}(i_c,t+2)$ due to mobility.

III. CHANNEL PREDICTION

The CSI from feedback can become outdated due to the relatively long feedback delay. We illustrate this with two examples in Fig. 2, where the real part of the fading process is plotted for 3 and 10 km/h in (a) and (b), respectively. ITU Pedestrian B model [20] and a 2.6 GHz carrier frequency are assumed. The sampling rate of the process is 200 Hz, which corresponds to the frame duration of 5 ms. The correlation coefficients between two samples 10 ms apart are 0.95 and 0.56 for 3 and 10 km/h, respectively. If a precoding matrix is selected for $\mathbf{H}(i_c,t)$, it is very likely that the matrix is not optimal for the actual channel $\mathbf{H}(i_c,t+2)$ that carries the precoded signal.

To mitigate the impact of feedback delay, SS predicts the channel response two frames ahead and selects the precoding matrix based on the prediction. While sophisticated parametric methods are available, e.g., [21], here we consider a simple non-

[1] An orthogonal matrix $\mathbf{A}$ has columns that are orthogonal each other and have unit norm, i.e., $\mathbf{A}^*\mathbf{A} = \mathbf{I}$. A Unitary matrix is a square orthogonal matrix with the same number of rows and columns.

parametric, linear filtering approach to reduce the implementation complexity. The optimal linear predictor is the Wiener filter [22]:

$$\mathbf{w} = \left(\mathbf{R}_h + \sigma^2\mathbf{I}\right)^{-1}\mathbf{p} \tag{2}$$

where $\mathbf{R}_h = \begin{bmatrix} r(0) & r(1) & \cdots & r(N_p-1) \\ r^*(1) & r(0) & \cdots & r(N_p-2) \\ \vdots & \vdots & \ddots & \vdots \\ r^*(N_p-1) & r^*(N_p-2) & \cdots & r(0) \end{bmatrix}$; $\mathbf{p} = \begin{bmatrix} r^*(2) & r^*(3) & \cdots & r^*(1+N_p) \end{bmatrix}^T$[2]; N_p is the number of filter taps. The autocorrelation is computed as $r(\tau) = \underset{i,j,i_c}{\mathrm{E}}\left[\mathbf{H}_{i,j}(i_c,t)\,\mathbf{H}^*_{i,j}(i_c,t+\tau)\right]$. The predicted channel is

$$\hat{\mathbf{H}}_{i,j}(i_c,t+2) = \mathbf{w}^*\mathbf{h} \tag{3}$$

where $\mathbf{h} = \begin{bmatrix} \mathbf{H}_{i,j}(i_c,t) & \cdots & \mathbf{H}_{i,j}(i_c,t-N_p+1) \end{bmatrix}^T$. The corresponding predication error is $\sigma_e^2 = r(0) - \mathbf{w}^*\mathbf{p}$. The inversion in (2) can be avoided by adaptive implementations such as LMS and RLS, which provide the additional benefit of tracking with windowing and forgetting factor [23]. The predicted channels of the previous examples are also plotted in Fig. 2. The impact of prediction error on packet error rate (PER) is hard to evaluate analytically, and we resort to numerical simulations in Section V.

IV. CODEBOOK STRUCTURE

In 802.16e system with up to 4 antennas and feedback sizes of 3 and 6 bits, there are fifteen combinations of N_t, N_s, and L, where L is the number of bits per feedback and 2^L is the codebook size. Since each combination requires a separate codebook, the storage of all codebooks is challenging for mobile devices. The codebooks we propose can be dynamically generated with low complexity. The set of codebooks is partitioned into vector and matrix codebooks, and each matrix codebook is generated from one or two vector codebooks using Householder reflection. Therefore, only the vector codebooks need to be stored. Vector codebook with $L = 3$ are optimized and stored directly because of small storage complexity. On the other hand, two large vector codebooks for 3×1, 4×1, and $L = 6$ are dynamically computed using Householder reflection and a modified Hochwald method for storage reduction.

A. Vector Codebook

Denote the channel matrix by $\mathbf{H}$. The beamforming matrix for a single stream is a vector, which uniformly distributes over a unit sphere due to symmetry of $\mathbf{H}$ with i.i.d. entries. The single stream transmission usually serves SS either with a single receive antenna or far from BS. Denote a codebook as $C(N_t, L)$, which is parameterized by N_t and L and has 2^L codewords. The five vector codebooks defined in 802.16e are $C(2,3)$, $C(3,3)$, $C(3,6)$, $C(4,3)$, and $C(4,6)$. Since the effective degrees of freedom for a 2×1 unit beamforming vector is only 2, 8 codewords, i.e., $L = 3$, are sufficient to cover the space. For $L = 3$, the unstructured vector codebooks are optimized using the chordal distance metric [4], [6], and are listed in section 8.4.5.4.10.14 of [1]. On the other hand, vector codebooks with 64 codewords result in storage issues and it is desirable to compute them dynamically in a structured manner. IEEE 802.16e adopted a method based on eigen-coordinate transformation. It improves the minimum chordal distance of the codebooks generated by the Hochwald method [4] (also called the block-circulant construction method). Hochwald method provides near-optimal codebooks with low storage since the parameterization of the codebook is very limited. The codebook is fully specified by the first codeword $\mathbf{V}_1$ and a diagonal rotation matrix $\mathbf{G}$. The other codewords are given by

$$\mathbf{V}_l = \mathbf{G}^{l-1}\mathbf{V}_1, \text{ for } l = 2,3,\cdots,2^L \tag{4}$$

where each codeword is $N_t \times N_s$ and $\mathbf{G} = \mathrm{diag}\left[e^{j\frac{2\pi}{2^L}u_1}, \cdots, e^{j\frac{2\pi}{2^L}u_{N_t}}\right]$ is specified by the integer vector $\mathbf{u} = [u_1, \cdots, u_{N_t}]$. Furthermore, $\mathbf{V}_1$ is chosen to be an $N_t \times N_s$ submatrix of the $N_t \times N_t$ DFT matrix $\mathbf{F}$, whose entry on the ith row and jth column is $e^{j\frac{2\pi}{N_t}(i-1)(j-1)}$. Therefore, $\mathbf{V}_1 = \begin{bmatrix} \mathbf{F}(:,k_1) & \cdots & \mathbf{F}(:,k_{N_s}) \end{bmatrix}$[3] is specified by the column index $[k_1, \cdots, k_{N_s}]$.

To improve upon the method of [4], we observe that the magnitude of each entry in each vector codeword remains constant because it equals to the corresponding entry in the first codeword $\mathbf{V}_1$ and $\mathbf{G}^{l-1}$ only change the phase of $\mathbf{V}_1$'s entry to obtain $\mathbf{V}_l$ in (4). The constant modulus is an unnecessary constraint that can be removed to achieve better chordal distance properties. We exploit the energy-shifting property of eigen-coordinate transformation while preserving some of the nice properties of the Hochwald codebook, such as easy parameterization, block-circulant distance distribution (i.e., $d(\mathbf{V}_i, \mathbf{V}_j) = d\left(\mathbf{V}_{\bmod(i+k,2^L)}, \mathbf{V}_{\bmod(j+k,2^L)}\right)$, where $d(\cdot,\cdot)$ is the chordal distance [26]), etc. The minimum chordal distance between any pair of codewords is systematically maximized by removing the constant modulus constraint.

Since $\mathbf{G}$ is diagonal, it can be viewed as a part of an eigen-decomposition of some Hermitian matrix $\mathbf{S}$:

$$\mathbf{S} = \mathbf{M}\,\mathbf{G}\,\mathbf{M}^* \tag{5}$$

where $\mathbf{M}$ is an $N_t \times N_t$ unitary matrix. We replace $\mathbf{G}$ by $\mathbf{S}$ in equation (4) as

$$\mathbf{V}_l = \mathbf{S}^{l-1}\mathbf{V}_1 = \left(\mathbf{M}\mathbf{G}\mathbf{M}^*\right)^{l-1}\mathbf{V}_1 = \mathbf{M}\mathbf{G}^{l-1}\mathbf{M}^*\mathbf{V}_1 \tag{6}$$

for $l = 2,3,\cdots,2^L$. The idea of the improved method is explained further in Fig. 3. To start the process, the first codeword $\mathbf{V}_1$ is transformed into the eigen-coordinates as $\mathbf{M}^*\mathbf{V}_1$, the Hochwald construction (4) is then applied on $\mathbf{M}^*\mathbf{V}_1$ to arrive at the lst codeword in the eigen-coordinate, $\mathbf{G}^{l-1}\mathbf{M}^*\mathbf{V}_1$, which is then transformed back to the Euclidean coordinate by $\mathbf{M}$ to give final output $\mathbf{V}_l = \mathbf{M}\mathbf{G}^{l-1}\mathbf{M}^*\mathbf{V}_1$. Although all the intermediate codewords $\mathbf{G}^{l-1}\mathbf{M}^*\mathbf{V}_1$ have the same energy distribution in the eigen-coordinates defined by $\mathbf{M}$, the final codewords $\mathbf{V}_l = \mathbf{M}\mathbf{G}^{l-1}\mathbf{M}^*\mathbf{V}_1$ have different energy distributions over

[2] * and ^{T} denote "conjugate transpose" and "transpose", respectively.

[3] The notation $\mathbf{A}_{:,i}$ denotes the ith column of matrix $\mathbf{A}$.

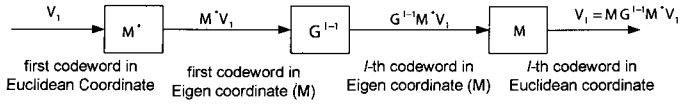

Fig. 3. Improved Hochwald method.

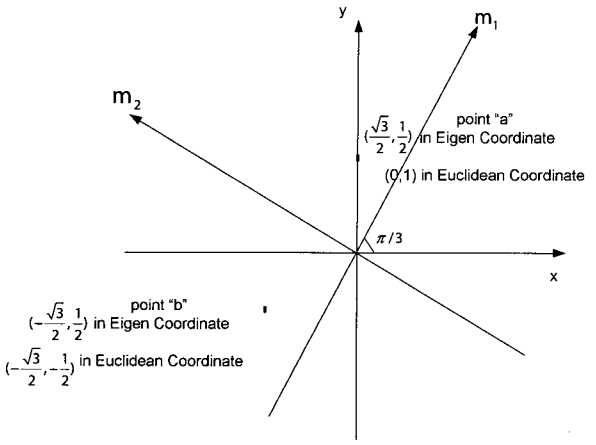

Fig. 4. Energy-shifting with eigen coordinate transformation. The energy distribution of points a and b are the same in eigen coordinate defined by and , but different in Euclidean coordinate.

the entries in the Euclidean coordinates. The idea of energy-shifting in eigen-coordinate transformation is illustrated in Fig. 4. The eigen-matrix $\mathbf{M}$ is parameterized. We further impose the Householder structure on $\mathbf{M}$ to allow a very simple parameterization of $\mathbf{M}$, i.e.,

$$\mathbf{M} = \mathbf{I} - 2\,\mathbf{b}\mathbf{b}^* \tag{7}$$

where $\mathbf{b}$ is an $N_t \times 1$ unit vector. We illustrate the effectiveness of the proposed method for several vector codebooks in Table 1. Since the minimum chordal distance of the improved Hochwald construction is greater than that of the original Hochwald construction, the improved construction results in a more uniform codeword distribution and thus a smaller average quantization error. We keep the first codeword $\mathbf{V}_1$ to be the first column of the DFT as in [4]. The only additional parameter we have added is the vector $\mathbf{b}$. However, we want to emphasize that our method also allows joint optimization over vector $\mathbf{b}$ and the first codeword $\mathbf{V}_1$ that can be any orthogonal matrix. It is worth noting that a global phase of each codeword is redundant, and we normalize the first entry of each codeword to be real. Later sections will use this property.

B. Matrix Codebook

The matrix codebooks are constructed using the vector codebooks as building blocks. We first consider the distribution of the optimal beamforming matrix and then design the codebook according to it. The singular value decomposition of $\mathbf{H}$ is

$$\mathbf{H} = \mathbf{U}\,\mathbf{\Sigma}\,\mathbf{V}^* \tag{8}$$

where $\mathbf{H}$ is $N_r \times N_t$; $\mathbf{U}$ is an $N_r \times N_r$ unitary matrix; $\mathbf{\Sigma}$ is an $N_r \times N_t$ diagonal matrix whose i-th diagonal entry is the i-th strongest singular value σ_i for $i = 1, \cdots, \min(N_r, N_t)$; and $\mathbf{V}$ is an $N_t \times N_t$ unitary matrix. The optimal beamforming scheme

Table 1. Codebooks based on improved Hochwald construction.

N_t	N_s	L	$\mathbf{u}$	$\mathbf{b}$	Chordal distance ratio: $\frac{\text{Propsed}}{[4]}$
3	1	6	$[1, 26, 57]$	$[0.2518-0.6409i,$ $-0.4570-0.4974i,$ $0.1177+0.2360i]$	$\frac{0.1263}{0.1166}$
4	1	3	$[1, 2, 7, 6]$	$[0.2895+0.3635i,$ $0.5287-0.2752i,$ $-0.2352-0.4247i,$ $-0.4040+0.1729i]$	$\frac{0.8282}{0.7500}$
4	1	6	$[1, 45, 22, 49]$	$[0.3954-0.0738i,$ $0.0206+0.4326i,$ $-0.1658-0.5445i,$ $0.5487-0.1599i]$	$\frac{0.3935}{0.3643}$

is the SVD beamforming [3], where the beamforming vectors are the columns of $\mathbf{V}$ and the gain of the i-th beamformed channel is σ_i. Adaptive transmit power loading can be conducted across the beamformed channels to achieve the closed-loop capacity. If the power adaptation selects only N_s beamformed channels to carry data, then feeding back the first N_s columns of $\mathbf{V}$ to the transmitter is sufficient. For channel with non-line of sight (NLOS) condition or large antenna spacing, the entries of $\mathbf{H}$ are modeled by i.i.d. circularly symmetric, complex, random variables with zero mean and unit variance. The distribution of $\mathbf{V}$, called Harr distribution, is uniform on the set of $N_t \times N_t$ unitary matrix, which is called Stiefel manifold and denoted by Ω_{N_t,N_t} [25]. The Harr distribution has a recursive property. It was stated in part in [10] and we sketch a proof in the appendix.

Proposition 1: Let $\mathbf{V}$ be uniformly distributed over Ω_{N_t,N_t} and $\mathbf{v}_1$ be the first column of $\mathbf{V}$. Furthermore, let $\mathbf{Q}(\mathbf{v}_1)$ be an $N_t \times N_t$ unitary matrix whose first row is $\mathbf{v}_1^*$ and rest of rows are independent of $\mathbf{V}$ except $\mathbf{v}_1$. Then, $\mathbf{v}_1$ is uniformly distributed over $\Omega_{N_t,1}$ and

$$\mathbf{Q}(\mathbf{v}_1)\,\mathbf{V} = \begin{bmatrix} 1 & \\ & \mathbf{V}_2 \end{bmatrix} \tag{9}$$

such that $\mathbf{V}_2$ is uniformly distributed over Ω_{N_t-1,N_t-1}.

Since both $\mathbf{V}$ and size-reduced $\mathbf{V}_2$ are uniformly distributed, it is possible to recursively quantize $\mathbf{V}$ column by column with decreasing dimensions. We may quantize the first column of $\mathbf{V}$ using a uniform vector codebook, reduce the problem size by one dimension, and recursively continue the quantization using another vector codebook with reduced dimension. Since only vector codebooks with uniform distribution are needed, the scheme is desirable for storage reduction and supports all antenna configurations including MISO. There are multiple choices for the unitary matrix $\mathbf{Q}(\mathbf{v}_1)$ satisfying Proposition 1. We choose Household reflection matrix for low complexity implementation and consistency with vector codebook construction in the previous subsection. Householder reflection matrix is defined as a unitary $N \times N$ matrix $\mathbf{Q}_{\mathrm{H}}(\mathbf{v})$ that is a

function of an $N \times 1$ unit vector $\mathbf{v}$:

$$\mathbf{Q}_{\mathrm{H}}(\mathbf{v}) = \begin{cases} \mathbf{I}, & \mathbf{v} = \mathbf{e}_1, \\ \mathbf{I} - \rho \mathbf{w}\mathbf{w}^*, & \text{otherwise} \end{cases} \tag{10}$$

where $\mathbf{v}$'s first entry is real; $\mathbf{w} = \mathbf{v} - \mathbf{e}_1$ and $\mathbf{e}_1 = [1\, 0 \cdots 0]^T$; $\rho = \frac{2}{\|\mathbf{w}^*\mathbf{w}\|}$; $\mathbf{I}$ is the $N \times N$ identity matrix; the first column and row of $\mathbf{Q}_{\mathrm{H}}(\mathbf{v})$ are $\mathbf{v}$ and $\mathbf{v}^*$, respectively. Since ρ is a real number that only depends on the input vector $\mathbf{v}$ and $\mathbf{v}$ is from a vector codebook, ρ can be pre-computed and stored and no division operation is needed in (10). Since $\mathbf{Q}_{\mathrm{H}}(\mathbf{v})$ is Hermitian, only N^2 real multiplications are needed. Therefore, the computation of (10) is of low complexity.

A recursive quantization scheme is illustrated in Fig. 5, where only the uniform vector codebooks in the previous subsection and Householder reflection are employed. There are four transmit and two receive antennas, respectively, in the downlink. The SS feeds back the first two columns of $\mathbf{V}$ to receive two data streams. The SS quantizes the first column of $\mathbf{V}$, $\mathbf{v}_1$, as

$$\hat{\mathbf{v}}_1 = \arg \max_{\mathbf{u} \in C_{4\times 1}} \|\mathbf{u}^* \mathbf{v}_1\| \tag{11}$$

where $C_{4\times 1}$ is the uniform 4×1 vector codebook in the previous subsection, $\hat{\mathbf{v}}_1$ has the maximum inner product among all unit vectors in the codebook. A Householder reflection matrix is constructed as

$$\mathbf{F}_1 = \mathbf{I} - \rho_1 \mathbf{w}_1 \mathbf{w}_1^* \tag{12}$$

where $\mathbf{w}_1 = \hat{\mathbf{v}}_1 - \mathbf{e}_1 = [\hat{v}_{11} - 1, \hat{v}_{21}, \hat{v}_{31}, \hat{v}_{41}]^T$ and $\rho_1 = \frac{2}{\|\mathbf{w}_1^* \mathbf{w}_1\|}$. If $\hat{\mathbf{v}}_1 = \mathbf{v}_1$, Householder reflection converts the first column and row of $\mathbf{V}$ into $[e^{j\phi_1}\, 0\, 0\, 0]^T$ and $e^{j\phi_1}[1\, 0]$ as shown in (13), where ϕ_1 is the phase of v_{11}. Since usually $\hat{\mathbf{v}}_1 \approx \mathbf{v}_1$, there will be nonzero residuals in the first column and row.

$$\mathbf{F}_1 \mathbf{V} = \begin{bmatrix} e^{j\phi_1} & 0.0 \\ 0.0 & \begin{bmatrix} \hat{v}_{11} \\ \hat{v}_{21} \\ \hat{v}_{31} \end{bmatrix} \\ 0.0 & \underbrace{\qquad\qquad}_{\mathbf{V}_2} \end{bmatrix} \tag{13}$$

where two properties are employed, i.e., $\hat{v}_{11}$ is real and $\mathbf{V}$ is orthogonal. Since both $\mathbf{F}_1$ is unitary and $\mathbf{V}$ is orthogonal, $\mathbf{V}_2$ is orthogonal. By Proposition 1 and the argument in its proof, $\mathbf{V}_2$ is uniformly distributed over $\Omega_{N_t-1,1}$. Seen from (13), the size of $\mathbf{V}_2$ is reduced from that of $\mathbf{V}$ by one row and one column. Recursively apply steps (11), (12), and (13), we quantize $\mathbf{V}_2$ using a 3×1 vector codebook. These steps are illustrated in Fig. 5. The quantization indexes q_1 and q_2 of $\mathbf{v}_1$ and $\mathbf{v}_2$ are fed back to BS. The BS computes the precoding matrix as shown in Fig. 6, where the indexes are converted to vectors by codeword lookup and the vectors are concatenated by Householder reflection with low complexity as explained below (10). It is worth noting that the phases ϕ_i are not needed for beamforming. The 4×2 matrix codebook in the example is effectively formed by the concatenation of 4×1 and 3×1 vector codebooks as shown in Fig. 6 by letting the q_1 and q_2 step through all the indexes.

Since the feedback sizes are fixed at 3 and 6 bits, the number of bits for each vector quantization is too small when three and more spatial channels are employed. As the number of codewords decreases per vector codebook, the performance of the recursive scheme degrades. 3 and 6 bits are not enough to describe each column of the ideal beamforming matrix, i.e., the first N_s columns of $\mathbf{V}$, but sufficient to specify the subspace spanned by the N_s columns. The set of the subspace is called Grassmann manifold [6], [25]. For $\mathbf{H}$ with i.i.d. entries, the subspace of the ideal beamforming matrix is uniformly distributed over Grassmann manifold. We present two schemes to quantize Grassmann manifold.

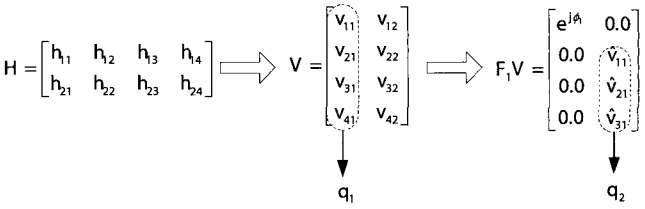

Fig. 5. Recursive quantization using vector codebooks.

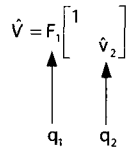

Fig. 6. Construction of beamforming matrix at transmitter using feedback indexes.

The feedback for $N_t \times (N_t - 1)$ beamforming matrices can be greatly reduced if SS feeds back the subspace instead of the exact beamforming matrix. It is noted that the subspace of the $N_t \times (N_t - 1)$ beamforming matrix is uniquely determined by its complementary, orthogonal space, which is an $N_t \times 1$ column vector as shown in Fig. 7. Therefore, only one, instead of $N_t - 1$, vector is quantized and fed back. When the strongest $N_t - 1$ singular values of the channel matrix are identical, there is no performance degradation for the complementary feedback. On the other hand, when the singular values of $\mathbf{H}$, are substantially different, the vector feedback causes interference between beamformed channels and also prevents efficient adaptive bit loading (ABL) and power loading at the transmitter. It results in a performance loss especially for linear receivers. For each $N_t \times (N_t - 1)$ orthogonal matrix $\mathbf{B}$, the complementary vector $\mathbf{v}$ is the norm vector of the subspace spanned by $\mathbf{B}$'s columns. Since the ideal $N_t \times (N_t - 1)$ beamforming matrix is uniformly distributed over the manifold, the norm vector is uniformly distributed in $\Omega_{N_t,1}$. The uniform vector codebook in the previous subsection can then be again used for the complementary scheme. The matrix codeword of the complementary scheme can be easily computed from that of the uniform vector codebook using Householder reflection. Let $\mathbf{v}$ be the vector codeword and $\mathbf{Q}_{\mathrm{H}}(\mathbf{v})$ be the Householder matrix computed by (10). It is noticed that the first column of $\mathbf{Q}_{\mathrm{H}}(\mathbf{v})$ is $\mathbf{v}$ and $\mathbf{Q}_{\mathrm{H}}(\mathbf{v})$ is an $N_t \times N_t$ unitary matrix. Then, column $2, \cdots, N_t$ forms an $N_t \times (N_t - 1)$ matrix codeword whose norm vector is $\mathbf{v}$. This approach can be generalized to efficiently generate codebooks for antenna configurations other than $N_t \times (N_t - 1)$. It reduces the number of vector codebooks to support the fifteen configura-

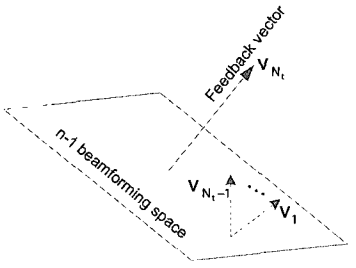

Fig. 7. Subspace spanned by the beamforming vectors $\mathbf{v}_1, \cdots, \mathbf{v}_{N_t-1}$ and the complementary feedback vector that is orthogonal to the subspace.

tions. For example, 4×2 codebook can be generated from 4×1 codebook by taking the first two columns of $\mathbf{Q}_{\mathrm{H}}(\mathbf{v})$, where $\mathbf{v}$ is from the 4×1 codebook.

For the $N_t \times N_t$ case, SS can still feed back only one vector, which corresponds to the weakest (or greatest) singular mode of $\mathbf{H}$. The feedback enables ABL on some beamformed channel and reduces the interference to the weakest channel (or the interference from the strongest channel). The $N_t \times N_t$ matrix codebook is computed from the uniform $N_t \times 1$ vector codebook using Household reflection (10), where the $N_t \times N_t$ codeword is $\mathbf{Q}_{\mathrm{H}}(\mathbf{v})$s and $\mathbf{v}$ is the vector codeword.

The generation of the matrix codebooks can be concisely represented by Householder operations. Each codeword in the vector codebook is complex with unit norm and the first entry is real. The first operation is the Householder reflection in (10). The other two operations are built on Householder reflection. One is called Householder concatenation while the other is called Householder expansion. Householder concatenation generates an $N \times (M+1)$ orthogonal matrix $\mathbf{Q}_{\mathrm{C}}(\mathbf{v}, \mathbf{A})$ from a unit $N \times 1$ vector $\mathbf{v}$ and an $(N-1) \times M$ orthogonal matrix $\mathbf{A}$ using Householder transformation as

$$\mathbf{Q}_{\mathrm{C}}(\mathbf{v}, \mathbf{A}) = \mathbf{Q}_{\mathrm{H}}(\mathbf{v}) \begin{bmatrix} 1 & \\ & \mathbf{A} \end{bmatrix} \tag{14}$$

where $N-1 \geq M$. Since the first and second terms on the right are unitary and orthogonal, respectively, $\mathbf{Q}_{\mathrm{C}}(\mathbf{v}, \mathbf{A})$ is orthogonal. The Householder expansion generates an $N \times l$ orthogonal matrix from an $N \times 1$ unit vector $\mathbf{v}$ by taking the last l columns of $\mathbf{Q}_{\mathrm{H}}(\mathbf{v})$ as

$$\mathbf{Q}_{\mathrm{E}}(\mathbf{v}, l) = \mathbf{Q}_{\mathrm{H}}(\mathbf{v})_{:, N-l+1:N}. \tag{15}$$

Three operations (10), (14), and (15) jointly generate matrix codebooks as shown in Table 2 and [1]. In Table 2, the vector codebook notation $C(N_t, L)$ in the input argument of the operations (i.e., $\mathbf{Q}_{\mathrm{H}}$, $\mathbf{Q}_{\mathrm{C}}$, and $\mathbf{Q}_{\mathrm{E}}$) denotes that each codeword in the vector codebook $C(N_t, L)$ is sequentially taken as an input parameter to the operations. The output of the operation is also a codebook. For example, in $\mathbf{Q}_{\mathrm{C}}(C(3,3), \mathbf{Q}_{\mathrm{H}}(C(2,3)))$, $\mathbf{Q}_{\mathrm{C}}$ has two codebooks as input. The first one is $C(3,3)$ with 8 vectors and the second one is $\mathbf{Q}_{\mathrm{H}}(C(2,3))$ with 8 2×2 matrices, which are computed from $C(2,3)$.

The performance loss due to the codebook quantization is not analyzed in this paper due to space limitation. The analysis can be conducted by following the frame work in [16]–[18]. The implementation complexity and feedback overhead are reported in [27] for a system similar to 802.16e, where the complexity of codebook quantization is below 1% of that of MMSE receiver.

Table 2. Generation operations of matrix codebooks.

N_t, L	2 streams	3 streams	4 streams
2, 3	$\mathbf{Q}_{\mathrm{H}}(C(2,3))$		
3, 3	$\mathbf{Q}_{\mathrm{E}}(C(3,3),2)$	$\mathbf{Q}_{\mathrm{H}}(C(3,3))$	
4, 3		$\mathbf{Q}_{\mathrm{E}}(C(4,3),3)$	$\mathbf{Q}_{\mathrm{H}}(C(4,3))$
3, 6	$\mathbf{Q}_{\mathrm{C}}(C(3,3), C(2,3))$	$\mathbf{Q}_{\mathrm{C}}(C(3,3), \mathbf{Q}_{\mathrm{H}}(C(2,3)))$	
4, 6	$\mathbf{Q}_{\mathrm{C}}(C(4,3), C(3,3))$	$\mathbf{Q}_{\mathrm{E}}(C(4,6),3)$	$\mathbf{Q}_{\mathrm{H}}(C(4,6))$

V. SIMULATIONS

We evaluate the proposed precoding scheme and compare it with other 802.16e MIMO schemes, i.e., STBC and antenna selection. The channel model is ITU Pedestrian B with NLOS condition and mobile speeds 3, 10, 15, and 20 km/h [20]. The numbers of transmit antennas are 2, 3, and 4. Transmit and receive antenna correlations are 0.2 and 0, respectively. The feedback delay is 2 frames, i.e., 10 ms. System bandwidth is 10 MHz and packet size is 512 bits. One codeword index is fed back per AMC band every 5 ms. Modulation levels are QPSK and 16 QAM, and coding scheme is convolutional codes with code rate $1/2$ and $2/3$. MMSE receiver is employed to detect multiple spatial streams. Two schemes use 3 bits per feedback, which are antenna selection and precoding with 3-bit codebook in [1]. Another precoding codebook uses 6 bits per feedback. For comparison purpose, the ideal SVD feedback is also simulated, where the exact SVD beamforming matrix for each subcarrier is sent back.

Since the ITU model has a maximum delay of 3700 ns and root mean square (RMS) delay of 750 ns, it causes significant frequency selectivity within the AMC band whose subcarriers share one common feedback. We employ the minimum mean square error (MSE) criterion in [6] and average over subcarriers of the AMC band in order to select the optimal precoding matrix for the band as

$$\mathrm{MSE}(\mathbf{V}_i) = \sum_{i_c=6,12,18,24,30} \mathrm{trace}\left(\left(\mathbf{I} + \gamma \mathbf{V}_i^* \mathbf{H}_{i_c}^* \mathbf{H}_{i_c} \mathbf{V}_i\right)^{-1}\right) \tag{16}$$

and

$$\mathbf{V}_{opt} = \arg \min_{\mathbf{V}_i \in C} \mathrm{MSE}(\mathbf{V}_i) \tag{17}$$

where $\mathbf{H}_{i_c}$ is the predicted channel for the i_cth subcarrier and five evenly spaced subcarriers over the band are evaluated, γ is the signal to noise ratio for each subcarrier. The performances are compared at PER 10%, which is a design target for some wireless systems.

We first evaluate the performance of the channel prediction scheme, where the 5-tap Wiener filter is employed for speed 3, 10, and 15 km/h and the 10-tap filter is employed for 20 km/h. The performances with and without channel prediction are shown in Fig. 8 for the 4×1 channel. The channel prediction

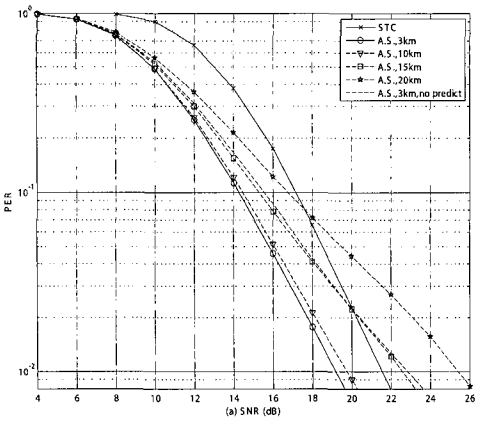

(a)

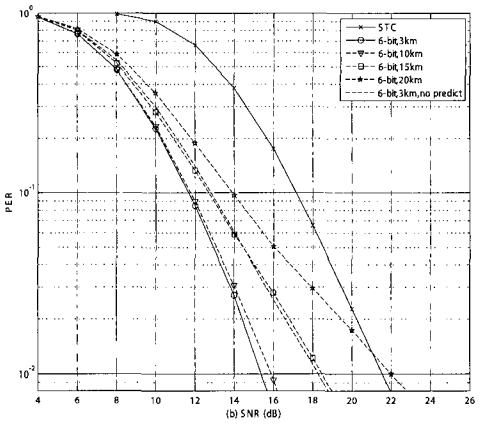

(b)

Fig. 8. PER performance of antenna selection and precoding at mobile speeds of 3, 10, 15, and 20 km/h. STBC performance is plotted as reference. The performance at 3 km/h without channel prediction is about the same as the performance at 15 km/h with channel prediction. Performance of antenna selection and precoding with 6 bit feedback are plotted in (a) and (b), respectively. The modulation and coding schemes are 16QAM and convolutional code with code rate $2/3$, respectively.

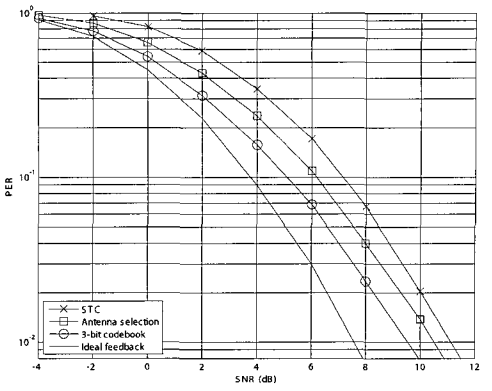

Fig. 9. PER performances of space-time code, i.e., Alamouti code, antenna selection, codebook based precoding, and ideal SVD precoding over 2×1 ITU Pedestrian B channels with 3 km/h mobile speed. The modulation and coding schemes are QPSK and convolutional code with code rate $1/2$, respectively.

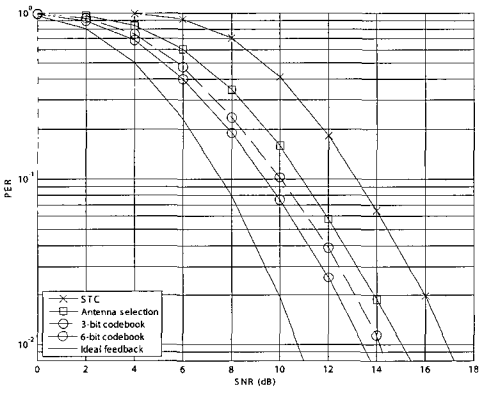

Fig. 10. PER performances of space-time code, antenna selection, codebook based precoding, and ideal SVD precoding over 3×1 ITU Pedestrian B channels with 3 km/h mobile speed. The modulation and coding schemes are 16QAM and convolutional code with code rate $1/2$, respectively.

delivers 1 dB gain at 3 km/h for antenna selection and precoding with 6-bit feedback. In addition, the performance with the channel prediction at 15 km/h is about the same as that without channel prediction at 3 km/h. At 20 km/h, the antenna selection, which consumes 3 bit per feedback, has about the same performance as that of STBC that doesn't need feedback. At the same speed and PER, precoding still outperforms STBC by 3.1 dB at the cost of 6 bits per feedback. Therefore, the channel prediction enables precoding to operate favorably at 20 km/h. The 5-tap channel prediction filter and 3 km/h mobile speed are assumed in the rest of performance analysis in order to be close to the practical usage model of precoding.

The performances of the vector codebooks are plotted in Figs. 9, 10, and 11 for antenna configurations 2×1, 3×1, and 4×1, respectively. Precoding with 3-bit feedback consistently outperforms antenna selection by about 1 dB for all three configurations. With 3 more feedback bits, 6-bit precoding provides an additional gain of 1.4 dB for 4×1. There is no 6-bit codebook defined for 2×1 in [1]. The STBC for 2×1 is the Alamouti code. The gain of precoding over STBC ranges from 2 to 5.5 dB across various antenna configurations. The frequency selectivity across the AMC band causes a 2 dB gap between the codebook based precoding and the ideal SVD.

The performances of the matrix codebooks are plotted in Figs. 12, 13, and 14 for antenna configurations 3×2, 4×2, and 4×3. Two spatial streams are sent in 3×2 and 4×2. Three streams are sent in 4×3 for antenna selection and precoding, while two streams are sent for STBC because there is no rate 3 STBC defined in [1] for four transmit antennas. The data rate of STBC with QPSK, code rate $2/3$, and two spatial streams are slightly lower than that of antenna selection and precoding with QPSK, code rate $1/2$, and three spatial streams. Note that the number of receive antennas are the same for all schemes. Precoding with 3-bit feedback consistently outperforms antenna selection by a fraction of a dB in these configurations. The gain of 6-bit pre-

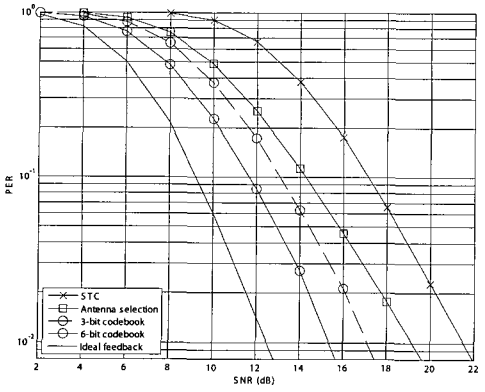

Fig. 11. PER performances of space-time code, antenna selection, codebook based precoding, and ideal SVD precoding over 4×1 ITU Pedestrian B channels with 3 km/h mobile speed. The modulation and coding schemes are 16QAM and convolutional code with code rate $2/3$, respectively.

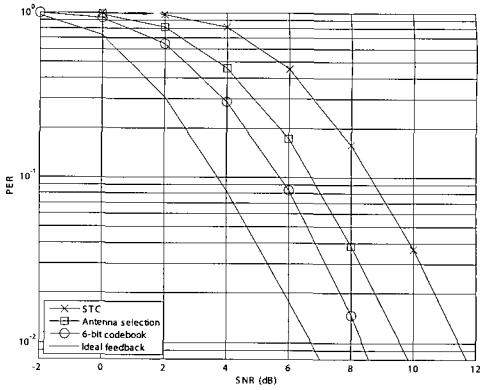

Fig. 13. PER performances of space-time code, antenna selection, codebook based precoding, and ideal SVD precoding over 4×2 ITU Pedestrian B channels with 3 km/h mobile speed. The modulation and coding schemes are QPSK and convolutional code with code rate $1/2$, respectively. Two spatial streams are sent.

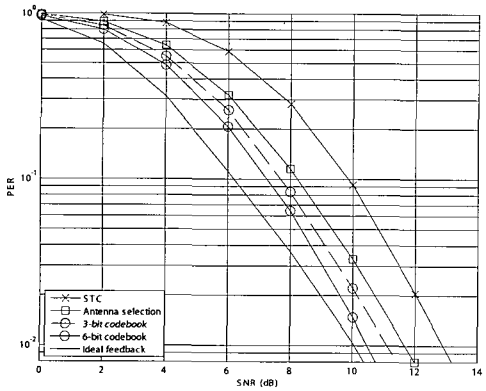

Fig. 12. PER performances of space-time code, antenna selection, codebook based precoding, and ideal SVD precoding over 3×2 ITU Pedestrian B channels with 3 km/h mobile speed. The modulation and coding schemes are QPSK and convolutional code with code rate $1/2$, respectively. Two spatial streams are sent.

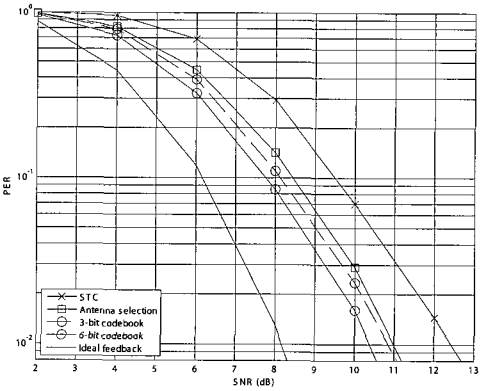

Fig. 14. PER performances of space-time code, antenna selection, codebook based precoding, and ideal SVD precoding over 4×3 ITU Pedestrian B channels with 3 km/h mobile speed. For antenna selection and precoding, the modulation and coding schemes are QPSK and convolutional code with code rate $1/2$, respectively, and three spatial streams are sent. Space-time code sends two streams with a comparable data rate.

coding over STBC ranges from 1.8 to 2.5 dB across the antenna configurations. Note that the PER curve slops of precoding and STBC are about the same for all antenna configurations. This implies that the precoding obtains both the beamforming gain and the diversity.

VI. CONCLUSIONS

The scalable transmit beamforming scheme for 802.16e WiMAX is described and compared with space-time coding and antenna selection. Fifteen antenna/feedback configurations are supported by a set of vector-based, structured codebooks with low storage complexity. The scheme outperforms antenna selection with the same system feedback and delivers a gain of more than 2 dB over open-loop space-time coding at the cost of 6 bit per feedback. A simple channel prediction enables the scheme to operate at 20 km/h with 10 ms feedback delay.

APPENDIX: PROOF OF PROPOSITION 1

Proof: Denote the first column of $\mathbf{V}$ by $\mathbf{v}_1$. First, we show that $\mathbf{v}_1$ is uniformity distributed by contradiction. Assume that there exists a $\mathbf{v}_1$ such that $p(\mathbf{v}_1) > p(\mathbf{e}_1)$, where $\mathbf{e}_1 = [1\ 0\ \cdots\ 0]^T$; $p()$ denotes the probability density function. Let $\mathbf{P}$ be an $N_t \times N_t$ unitary rotation that transforms $\mathbf{e}_1$ to $\mathbf{v}_1$ and $\mathbf{v}_1$ to $\mathbf{e}_1$, e.g., Household reflection. Let's consider the set of the first columns of $\mathbf{PV}$, where $\mathbf{P}$ is fixed and $\mathbf{V}$ is uniform over the manifold. Since $\mathbf{PV}$ rotates the whole distribution, we have $p(\mathbf{e}_1) = p(\mathbf{Pv}_1) > p(\mathbf{Pe}_1) = p(\mathbf{v}_1)$, i.e., $p(\mathbf{e}_1) > p(\mathbf{v}_1)$ for $\mathbf{PV}$. However, since the joint column distribution of $\mathbf{V}$ and $\mathbf{PV}$ are the same due to the rotation invariance property of Harr distribution [25], the marginal distributions should be the same with and without the rotation, i.e., $p(\mathbf{v}_1) > p(\mathbf{e}_1)$ for $\mathbf{PV}$. Similarly, we can assume $p(\mathbf{v}_1) < p(\mathbf{e}_1)$ and draw the contradiction. This proves that $\mathbf{v}_1$ is uniformly distributed.

For the second part, it is easy to check that

$$\mathbf{V}\,\mathbf{Q}_{\mathrm{H}}(\mathbf{v}_1) = \begin{bmatrix} 1 & \\ & \mathbf{V}_2 \end{bmatrix} \tag{A-1}$$

where the zeros in the first row and column are due to unitary property of $\mathbf{V}$. By the chain rule, the probability density function of $\mathbf{V}$ is given by $p(\mathbf{V}) = p(\mathbf{V}_2, \mathbf{v}_1) = p(\mathbf{v}_1)\,p(\mathbf{V}_2 \,|\mathbf{v}_1)$. Since $p(\mathbf{V})$ is constant due to uniformity of Harr distribution and the marginal $p(\mathbf{v}_1)$ is constant as shown above, $p(\mathbf{V}_2 \,|\mathbf{v}_1)$ is constant and thus $\mathbf{V}_2$ is uniformly distributed. In the proof above, $\mathbf{Q}_{\mathrm{H}}(\mathbf{v}_1)$ can be replaced by any unitary matrix whose first row is $\mathbf{v}_1^*$ and the rest of rows are independent of the columns of $\mathbf{V}$ except $\mathbf{v}_1$. □

ACKNOWLEDGEMENTS

The coauthors would like to thank Ada Poon, June Chul Roh, and Alexei Davydov for helpful discussions.

REFERENCES

[1] IEEE 802.16e-2005 and IEEE Std 802.16-2004/Cor 1-2005, *IEEE standard for local and metropolitan area networks, Part 16: Air interface for fixed and mobile broadband wireless access systems*, Feb. 28, 2006.

[2] IEEE 802.16-2004, *IEEE Standard for local and metropolitan area networks, Part 16: Air interface for fixed broadband wireless access systems*, Oct. 1, 2004.

[3] I. E. Telatar, "Capacity of multi-antenna Gaussian channels," AT&T Bell Labs Tech. Memo., 1995.

[4] B. M. Hochwald, T. L. Marzetta, T. J. Richardson, W. Sweldens, and R. Urabanke, "Systematic design of unitary space-time constellations," *IEEE Trans. Inf. Theory*, vol. 46, pp. 1962–1973, Sept. 2000.

[5] E. N. Onggosanusi and A. G. Dabak, "A feedback-based adaptive multi-input multi-output signaling scheme," in *Proc IEEE Asilomar Conf.*, vol. 2, Nov. 2002, pp. 1694–1698.

[6] D. J. Love and R. W. Heath Jr., "Limited feedback precoding for spatial multiplexing systems," in *Proc. IEEE GLOBECOM*, vol. 4, Dec. 2003, pp. 1857–1861.

[7] R. W. Heath, J. Chiang, B. Mondal, and R. Samanta, "11n partial proposal: Quantized precoding with feedback," IEEE P802.11n-04/962, Aug. 2004.

[8] B. Mondal, B. R. Samanta, and R. W. Heath Jr., "Frame theoretic quantization for limited feedback MIMO beamforming systems," in *Proc. IEEE ICWCMC*, vol. 2, June 2005, pp. 1065–1070.

[9] J. C. Roh and B. D. Rao, "An efficient feedback method for MIMO systems with slowly time-varing channels," in *Proc. IEEE WCNC*, vol. 2, Mar. 2004, pp. 760–764.

[10] J. C. Roh and B. D. Rao, "Channel feedback quantization methods for MISO and MIMO systems", in *Proc. IEEE PIMRC*, vol. 2, Sept. 2004, pp. 805–809.

[11] Q. Li and X. E. Lin, "Compact feedback for MIMO-OFDM systems over frequency selective channels", in *Proc. IEEE VTC 2005-spring*, vol. 1, May-June. 2005, pp. 187–191.

[12] Q. Li, X. E. Lin, A. Poon, M. Ho, N. Himayat, and S. Talwar, "Improved feedback for MIMO precoding," IEEE C802.16e-04/527r4, Nov. 2004.

[13] J. Zhang, H. Zhang, N. V. Waes, A. Reid, and V. Stolpman, "Closed-loop MIMO precoding with limited feedback," IEEE C802.16e-04/262r1, Aug. 2004.

[14] M. Ikram, E. N. Onggosanusi, V. Raghavan, et al., "An enhanced closed-loop MIMO design for OFDM/OFDMA-PHY," IEEE C802.16e-04/267, Aug. 2004.

[15] Q. Li, X. E. Lin, A. Poon, A. Davydov, U. Perlmutter, M. Ho, N. Himayat, R. Schwartz, and J. Puthenkulam, "Compact codebooks for transmit beamforming in closed-loop MIMO," IEEE C802.16e-04/50r6, Jan. 2005.

[16] P. Xia and G. B. Giannakis, "Design and analysis of transmit-beamforming based on limited-rate feedback," *IEEE Trans. Signal Process.*, vol. 54, no. 5, pp. 1853–1863, May 2006.

[17] J. Zheng and B. D. Rao, "Capacity analysis of multiple antenna systems with mismatched channel quantization schemes," in *Prco. ICASSP*, vol. 4, May 2006, pp. 85–88.

[18] J. C. Roh and B. D. Rao, "Design and analysis of MIMO spatial multiplexing systems with quantized feedback," *IEEE Trans. Signal Process.*, vol. 54, no. 8, pp. 2874–2886, Aug. 2006.

[19] Y. Hassan, "Scalable OFDMA physical layer in IEEE 802.16 WirelessMAN," *Intel Technol. J.*, vol. 8, pp. 201–212, Aug. 2004.

[20] *Recommendation ITU-R M.1225*, "Guidelines for evaluation of radio transmission technologies for IMT-2000," 1997.

[21] Y. Lee, "Channel prediction with cascade AR modeling," in *Proc. IEEE AICT-ICIW*, Feb. 2006, p. 40.

[22] H. V. Poor, *An Introduction to Signal Detection and Estimation*, 2nd ed. Springer, 1994.

[23] S. Haykin, *Adaptive Filter Theory*, 3rd ed. Prentice-Hall Inc., 1996.

[24] G. Golub and C. Van Loan, *Matrix Computations*, 3rd ed. Johns Hopkins University Press, 1996.

[25] R. J. Muirhead, *Aspects of Multivariate Statistical Theory*. John Wiley, Inc., 1982.

[26] J. H. Conway, R. H. Hardin, and N. J. A. Sloane, "Packing line, planes, etc.: Packings in Grassmannian spaces," *Experimental Mathematics*, vol. 5, pp. 139–159, 1996.

[27] Intel Corporation, "Scaleable Precoding and Implementation Complexities," *3GPP TSG RAN WG1 meeting 45*, R1-061126, May 2006.

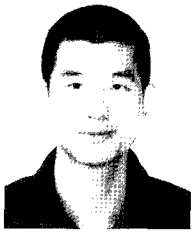

Qinghua Li received the B.E. degree in Radio Engineering from South China University of Technology, Guangzhou, China, the M.E. degree in Signal Processing from Tsinghua University, Beijing, China, and the Ph.D. degree in Electrical Engineering from Texas A&M University, College Station, Texas, in 1992, 1995, and 2001, respectively. From 1995 to 1996, he was with Guangdong Telecommunication Academy of Science and Technology, China, where he was involved in the development of telephone exchange networks. Since February 2001, he has been with the wireless research group of Intel Corporation, Santa Clara, CA. His research interests are in the areas of MIMO, SDMA, relay network, ultra-wide band communications, wireless channel modeling, multiuser detection, interference mitigation, channel coding, and media access control protocols.

Xintian Eddie Lin was born in Chengdu, China on July 1, 1969. He received the B.S. degree in Physics from the University of Science and Technology of China in 1988. He then obtained the M.S. and the Ph.D. degrees in Physics from University of California, San Diego in 1989 and 1995, respectively. From April 1995 to September 2000, he was a research staff and postdoc fellow at Stanford Linear Accelerator Center, Stanford University. In October 2000, he joined Intel and became a wireless communication architect. He is currently a principal engineer in Mobility Group. His major interest is in the area of electromagnetic theory, photonic bandgap material and digital wireless communications, especially MIMO OFDM close loop feedback. His recently work includes IEEE 802.16e standard contributions on channel state feedback, compact antennas, platform RF noise mitigation and radio coexistence on notebook platform.

Jianzhong (Charlie) Zhang received the B.S. degrees in both Electrical Engineering and Applied Physics from Tsinghua University, Beijing, China in 1995, the M.S. degree in Electrical Engineering from Clemson University in 1998, and the Ph.D degree in Electrical Engineering from University of Wisconsin at Madison in May 2003. He is currently a senior staff engineer with Samsung. Before he joined Samsung, he was a principal staff engineer with Motorola, and was the technical lead of the 3GPP HSPA standardization effort, focusing on areas such as MBMS, VoIP optimization, MIMO, etc. He also worked with Nokia from June 2001 to March 2006, where he was a senior research engineer and lead Nokia's phyical layer contribution to the IEEE 802.16e standard on topics such as LDPC codes, space-time-frequency coding and limited feedback based MIMO precoding.